

Energy Efficient Coils for Magnetic Stimulation of Peripheral Nerves

Laura Darabant¹, Mihaela Plesa¹, Dan D. Micu¹, Denisa Stet¹, Radu Ciupa¹, and Adrian Darabant²

¹Electrotechnics Department, Technical University of Cluj-Napoca, 15 Ctin Daicoviciu, Cluj-Napoca, Romania

²Computer Science Department, Babes-Bolyai University, Cluj-Napoca, Romania

The preoccupation for improving the quality of life, for persons with different handicaps, led to extended research in the area of functional stimulation. Due to its advantages compared to electrical stimulation, magnetic stimulation of the human nervous system is now a common technique in modern medicine. A difficulty of this technique is the need for accurate focal stimulation. Another one is the low efficiency of power transfer from the coil to the tissue. To address these difficulties, coils with special geometries must be designed.

Index Terms—Coil design, energetic efficiency, magnetic stimulation, nervous system.

I. INTRODUCTION

THE preoccupation for improving the quality of life, for persons with different handicaps, led to extended research in the area of functional stimulation.

The human nervous system can be stimulated by strong magnetic field pulses that induce an electric field in the tissue, leading to excitation of neurons [1]. A disadvantage consists, however, in the fact that the need of focal stimulation can not always be fulfilled. This is why the design of magnetic coils can help achieving this goal.

The present paper starts by emphasizing the theoretical background of magnetic stimulation, referring to the mathematical model for the computation of the electric field, the electric circuit of the stimulator and the computation of the inductivity of magnetic coils. Then, for coils of optimal shape, that provide an improved focality of the stimulation—Slinky coils—we analyze where the turns should be placed, inside the coil, to achieve activation with minimum energy cost.

II. THEORETICAL BACKGROUND

The current required to induce the electric field (high field strength are required in magnetic stimulation) is delivered by a magnetic stimulator (RLC circuit). The current waveform through the discharging of a capacitor, with an initial voltage U_0 , to the coil is [2]

$$I = U_0/\omega L \cdot \sin(\omega t) \exp(-\alpha t) \quad (1)$$

where $\alpha = R/(2L)$, $\omega = \sqrt{1/LC - \alpha^2}$, C is the capacitance, and R and L are the resistance and inductance of the coil, respectively.

According to the electromagnetic field theory, the electric field \vec{E} can be computed as a function of the electric potential V and the magnetic vector potential [2]

$$\vec{E} = -\frac{\partial \vec{A}}{\partial t} - \text{grad } V. \quad (2)$$

Manuscript received October 07, 2008. Current version published February 19, 2009. Corresponding author: L. Darabant (e-mail: laura.darabant@et.utcluj.ro).

Color versions of one or more of the figures in this paper are available online at <http://ieeexplore.ieee.org>.

Digital Object Identifier 10.1109/TMAG.2009.2012783

The first term of (2), called “primary electric field— \vec{E}_A ”, is determined by means of the magnetic vector potential. For coils of non-traditional shapes, one can compute \vec{A} using an approximation method in which the contour of the coil is first divided into a variable number of equal segments, and the magnetic vector potential in the calculus point is obtained by adding the contribution of each segment to the final value [2], [3].

Considering the notations in Fig. 1 and the fact that the current $I(t)$ flows through the conductor, the magnetic vector potential created by the segment into point P can be written, using the vectors defined above, as

$$\vec{A} = \frac{\mu_0 I(t)}{4\pi} \cdot \frac{\vec{l}}{l} \cdot \ln \frac{|\vec{l} - \vec{r}| + l - \frac{l\vec{r}}{l}}{r - \frac{l\vec{r}}{l}}. \quad (3)$$

The second term of (4) represents “the secondary electric field - \vec{E}_V .” It depends on the geometry of the tissue-air boundary. A common application of magnetic stimulation is to excite peripheral nerves [3]. The tissue-air interface is considered a flat surface. This term is computed knowing that on the surface, the boundary condition to be fulfilled is: $\vec{n} \cdot \vec{E}_A = -\vec{n} \cdot \vec{E}_V$ (continuity of the normal component of the current density vector, valid considering the fact that the regime of the electromagnetic field is quasistatic ($f < 1000$ Hz) and therefore the time variation of the charge accumulated on the tissue-air boundary is zero). The electric field created by a flat surface charged with a certain charge density is $\vec{E} = \rho_S/2\epsilon_r\epsilon_0$, and the charge accumulation occurs until the normal component of the primary electric field equals the normal component of the secondary electric field; therefore one can compute ρ_S as $\rho_S = -2 \cdot \epsilon_r \cdot \epsilon_0 \cdot \vec{n} \cdot \vec{E}_A$.

One of the major problems that appear in the design phase is the computation of the inductivity of the stimulating coil. For simple shapes of the coils (circular), one can determine analytical computation formulas. When, however, the shape and the spatial distribution of the coil’s turns do not belong to one of the known structures, a numerical method needs to be used for determining the inductivity.

The inductance is evaluated by taking the line integral of the vector potential around the coil, for unit current [4]: $L = \oint \vec{A} \cdot d\vec{l}$. This formula permits the computation of inductances of the special coils, designed to improve focality.

The idea is to divide the coils in small portions. Starting from this method, two computation systems were developed by the authors of this paper.

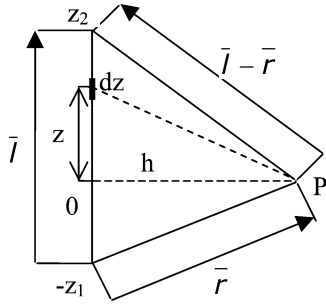


Fig. 1. Notation for the computation of the magnetic vector potential produced by a conductor segment.

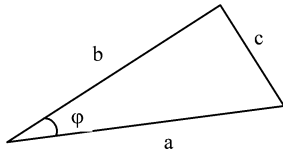


Fig. 2. Computing the mutual inductivity between two converging conductors.

- The first one is classical and it just consists of a software implementation (Matlab);
- The second one consists of realizing a hardware architecture that exploits the intrinsic parallelism of the problem. The physical support of this architecture is an FPGA device.

The problem with the software implementation is its running time. Coils are designed by trial-and-error, and this approach is impractical if each trial requires half a day of computation. Besides, as this time grows with the complexity of the coil, it prevents designing complex coils. The FPGA-based hardware acceleration is able to solve this bottleneck [5].

The self-inductance of the circuit, divided in n parts, can be computed with formula (4). This mainly adds up the self-inductivities of the separate segments with the mutual inductivities of all the involved segments [6]

$$L = \sum_{k=1}^n L_k + \sum_{k=1}^n \sum_{i=1}^n M_{ki}, \text{ for } (i \neq k). \quad (4)$$

The self inductivity of a short straight conductor, with round cross-section, for low frequencies, is [6]

$$L = \frac{\mu_0 l}{2\pi} \left(\ln \frac{2l}{r} - \frac{3}{4} + \frac{128 r}{45\pi l} - \frac{r^2}{4l^2} \right) \quad (5)$$

with l the length of the conductor, and r the radius of its cross-section.

The mutual inductivity between two straight conductors converging into a point is evaluated as [6]

$$M = \frac{\mu_0}{4\pi} \cos \varphi \left[a \ln \frac{a+b+c}{c+a-b} + b \ln \frac{a+b+c}{c+b-a} \right]. \quad (6)$$

The given quantities are represented in Fig. 2, with a and b representing the length of the conductors and φ the angle between them.

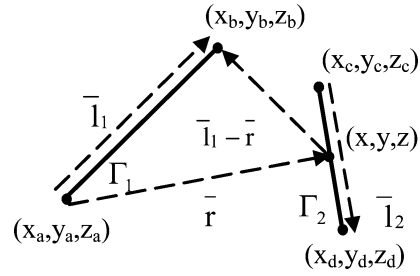


Fig. 3. Two segments in space.

For the general case, we consider two conductor segments in space. The first segment is between points of coordinates (x_a, y_a, z_a) and (x_b, y_b, z_b) , while the second segment is between points (x_c, y_c, z_c) and (x_d, y_d, z_d) , see Fig. 3.

On the second segment, we consider a point of coordinates (x, y, z) . The parametric equation of the second segment is

$$\begin{cases} x(s) = x_c + (x_d - x_c) s \\ y(s) = y_c + (y_d - y_c) s \\ z(s) = z_c + (z_d - z_c) s \end{cases} \quad (7)$$

With the above geometrical coordinates, we can find the mutual inductivity between these segments (using Neumann formula). For two circuits, Γ_1 and Γ_2 , in a homogenous media with permeability μ , the mutual magnetic flux Φ_{21} is

$$\Phi_{21} = \int_{S_{\Gamma_2}} \bar{B}_{21} d\bar{S} = \int_{\Gamma_2} \bar{A}_{21} d\bar{l}_2. \quad (8)$$

Since circuits Γ_1 and Γ_2 are shaped like two straight segments, the mutual flux can be evaluated by integrating the magnetic vector potential created by the first segment along the second one. Considering the magnetic vector potential generated by a conductor segment (see (3)), the mutual inductivity can be computed using the following:

$$L_{21} = \frac{\mu_0}{4\pi} \cdot \oint_{\Gamma_2} \ln \frac{|\bar{l}_1 - \bar{r}| + l_1 - \frac{\bar{l}_1 \cdot \bar{r}}{l_1}}{r - \frac{\bar{l}_1 \cdot \bar{r}}{l_1}} \cdot \frac{\bar{l}_1}{l_1} \cdot d\bar{l}_2. \quad (9)$$

The vectors in (9) are

$$\begin{aligned} d\bar{l}_2 &= (x'(s) \cdot \bar{i} + y'(s) \cdot \bar{j} + z'(s) \cdot \bar{k}) \cdot ds \\ &= ((x_c - x_d) \cdot \bar{i} + (y_c - y_d) \cdot \bar{j} + (z_c - z_d) \cdot \bar{k}) \cdot ds \\ \bar{l}_1 &= (x_b - x_a) \cdot \bar{i} + (y_b - y_a) \cdot \bar{j} + (z_b - z_a) \cdot \bar{k} \\ \bar{r} &= (x(s) - x_a) \cdot \bar{i} + (y(s) - y_a) \cdot \bar{j} + (z(s) - z_a) \cdot \bar{k} \\ \bar{l}_1 - \bar{r} &= (x_b - x(s)) \cdot \bar{i} + (y_b - y(s)) \cdot \bar{j} + (z_b - z(s)) \cdot \bar{k} \end{aligned}$$

while coordinates x, y, z are expressed as a function of parameter s , according to (7). The limits of the integral in (9) are given by $s \in [0, 1]$.

In order to assess the efficiency of energy transfer from the stimulator to the target biological tissue, we focus on stimulators with a fixed rise time of the current $I(t)$ from 0 to peak, which is sufficient for comparing relative figures of merit of the stimulators.

The value of the coil's inductance, L , can be evaluated with the algorithm described above. The coil's resistance is

$$R = 2\pi\eta A^{-1} \sum_{i=1}^N r_i. \quad (10)$$

where A is the cross-sectional area, η the resistivity of the wire and r_i the radius of the i th loop.

Given the values of L and R , the capacitance C is obtained requiring that the rise time of the current is fixed ($\tau = 70 \mu\text{sec}$).

Because of the same requirement, we may substitute dI/dt [from (3)] with $dI/dt_{t=0} = U_0/L$. Assuming that the activation of the nerve fiber occurs for a preset value of the electric field E , we obtain U_0 , the necessary initial voltage on the capacitor that would lead to activation.

The energy dissipated in the circuit during one pulse of duration Δt is [1]

$$W_J = R \int_0^{\Delta t} I^2(t) dt. \quad (11)$$

The peak magnetic energy in the coil W_B required to induce a given electric field is [1]

$$W_B = \frac{1}{2} L I_{\text{peak}}^2. \quad (12)$$

The temperature rise in the coil after one pulse of duration Δt is (assuming there is no cooling) [1]

$$\Delta T = \frac{\eta}{c\sigma A^2} \int_0^{\Delta t} I^2(t) dt. \quad (13)$$

where η is the resistivity, σ the density, c the specific heat and A the cross-sectional area of the copper wire of the coil.

These three quantities are evaluated to establish the parameters of energy transfer from the coil to the target tissue.

III. RESULTS AND DISCUSSIONS

Considering a coil with N turns, the "Slinky- k " coils are generated by spatially locating these turns at successive angles of $i \times 180/(k-1)$ degrees, where $i = 0, 1, \dots, k-1$ [3]. If the current passing through this coil is I , then the central leg carries the total current $N \times I$. With this definition, the circular coil is considered a "Slinky-1" coil, and the figure of eight is a "Slinky-2" coil.

For a circular coil, and then for our specially designed Slinky-4 coils, we tried to establish how the dimensions and position of the turns (the coil profile) influence its energetic parameters.

First, we estimated the strength of the induced electric field at the target due to a single filamentary loop. The loop's radius is r , and its distance from the target point is d —see Fig. 4. The target is at radial distance R from the loop's axis. The rate of change of current is assumed to be $100 \text{ A}/\mu\text{s}$, and the plot is given in Fig. 5.

From Fig. 5 one can conclude that the largest loop nearest the target induces the larger electric field. Therefore, for simple circular coils, the coil profile should mimic the behavior of Fig. 5

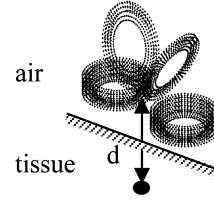


Fig. 4. Slinky_4 coil and the target point. The distance from the coil to the tissue-air interface is 5 mm in all cases.

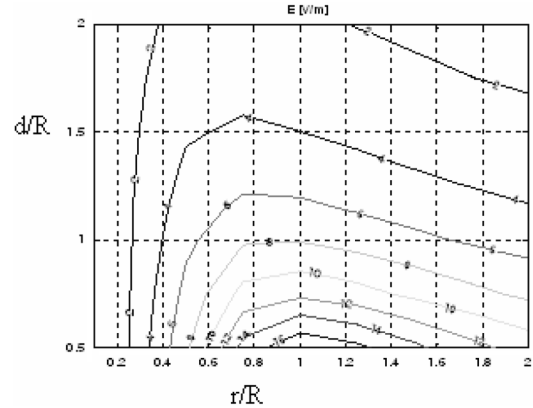


Fig. 5. Strength of the induced electric field at the target point due to a single filamentary loop.

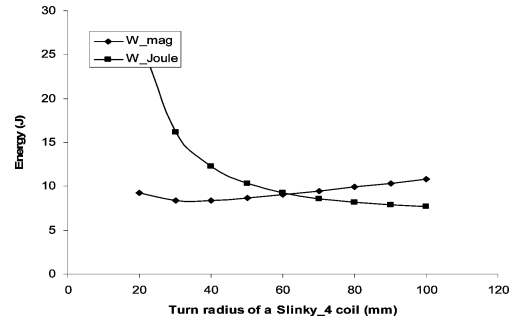


Fig. 6. Variation of energy consumed by a Slinky_4 coil as a function of leaf radius.

(i.e., the number of turns should decrease with the level distance from the target).

Considering the previous conclusion, we tried to establish how the coil profile of a Slinky-4 influences its energetic parameters.

For a Slinky-4 coil, 3-1-1-3 turns/leaf, the computations were performed considering that activation occurs when the value of the electric field induced in the target point reaches the value of 100 V/m . We computed the total electric field 5 mm below the tissue-air interface (the total distance from the coil to the target point is 10 mm), and we evaluated the variation of the Joulean and magnetic energy, as a function of the radius of the leaf. Results are depicted in Fig. 6, and one can see that the optimal value of this radius—the one that leads to the lowest energy consumption—is about 30 mm. For this value, the magnetic energy consumed is minimum, and although the Joulean energy still decreases as the radius increases, this decrease is no longer significant.

Then, we considered 25 different configurations of a larger Slinky_4 coil. All these configurations respect the structure of the previous Slinky-4 coil (established to produce a more focal

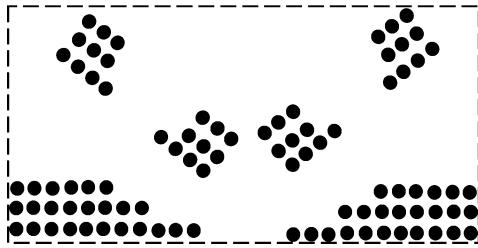


Fig. 7. The inner structure of an optimized Slinky-4 coil (the one highlighted in Table I).

TABLE I
ENERGETIC PARAMETERS OF A SET OF SLINKY-4 COILS, ON 25 DIFFERENT GEOMETRICAL CONFIGURATIONS

Configuration	L (μH)	C (μF)	I _{peak} (A)	W _J (J)	W _B (J)	ΔT ($^{\circ}\text{C}$)
5,5,5,5,5 – 5,5	100,3	20.258	369.5642	1.4882	6.8494	0.0094
5,5,5,5,5 – 4,3,3	103,7	19.586	362.4022	1.4527	6.8097	0.0090
7,6,6,6 – 5,5	93,3	21,8	357.7678	1.3524	5.9711	0.0088
7,6,6,6 – 4,3,3	98,7	20.587	350.1528	1.3165	6.0507	0.0084
8,7,5,5 – 5,5	90,8	22.412	360.2231	1.3624	5.8911	0.0089
8,7,5,5 – 4,3,3	96,2	21.132	352.5096	1.3261	5.9770	0.0085
8,7,6,4 – 5,5	90,3	22.538	361.0413	1.3659	5.8853	0.0089
8,7,6,4 – 4,3,3	93,8	21.685	353.2233	1.3280	5.8516	0.0086
8,7,7,3 – 5,5	89,5	22.741	363.7414	1.3784	5.9208	0.0091
8,7,7,3 – 4,3,3	91,7	22.191	355.7584	1.339	5.803	0.0087
9,7,5,4 – 5,5	89,1	22.846	364.6786	1.3853	5.9247	0.0091
9,7,5,4 – 4,3,3	93,3	21.801	356.7318	1.347	5.9366	0.0087
10,5,5,5 – 5,5	86,3	23.604	368.3421	1.4067	5.8544	0.0093
10,5,5,5 – 4,3,3	91,7	22.186	360.3239	1.3611	5.9529	0.0089
10,6,6,3 – 5,5	84,6	24.087	370.9473	1.4179	5.8206	0.0094
10,6,6,3 – 4,3,3	88	23.142	362.6989	1.3773	5.7882	0.0090
11,8,6 – 5,5	76,7	26.61	364.9574	1.3175	5.108	0.0091
11,8,6 – 4,3,3	80,3	25.403	355.7643	1.2859	5.0817	0.0087
10,8,7 – 5,5	79,1	25.786	365.0187	1.3294	5.2696	0.0091
10,8,7 – 6,4	78,5	25.987	365.891	1.3329	5.2546	0.0092
10,8,7 – 4,3,3	82,8	24.621	355.8257	1.2973	5.2417	0.0087
9,8,8 – 5,5	80,4	25.361	363.0393	1.3207	5.2983	0.0090
9,8,8 – 4,3,3	84,1	24.233	353.9403	1.289	5.2678	0.0086
10,9,6 – 5,5	77,8	26.226	367.5051	1.3417	5.2538	0.0092
10,9,6 – 4,3,3	83,4	24.43	358.3462	1.2981	5.3548	0.0088

induced electric field [4]), having more turns on the horizontal leafs (leafs 1 and 4) than on the bended ones (leafs 2 and 3). In all cases, there are 25 turns on each of the two horizontal directions and 10 turns on each of the two bended ones (a total number of 70 turns). These larger coils are necessary since most stimulators require that the coil's inductivity is above 50 μH . Such a coil will have several turns, and therefore computing the inductivity is a very long process using the software implementation of our algorithm. But the hardware one is able to solve this problem.

The geometrical parameters of the coil are: outer radius–30 mm, wire radius–1 mm and insulation gap between turns–0, 2 mm. Considering now that the activation threshold is set to 60 V/m in the target point—positioned 10 mm under the center of the coil, Table I presents the energetic parameters evaluated for these coils. The configuration section of Table I gives only the number of turns and levels for the first and second leafs of the Slinky-4 coil. Leaf 3 is symmetrical with leaf 2 and leaf 4 is symmetrical with leaf 1. For example, the optimal coil, highlighted,

has, on the first leaf: 11 turns on the first level, 8 turns on the second one and 6 turns on the third level; on the second leaf, we have: 4 turns on the first level, and 3 on the second and the third one; Fig. 7 gives a better understanding of the position of the turns inside the coil.

One can see that the space distribution of the turns can play a very important role on improving the energy transfer from the coil to the tissue. One can observe that the energy dissipated in the circuit is 15% lower for the most efficient configuration than for the less efficient one, and the coil heating per pulse is also 8% smaller. The optimal coil structure of turns is plotted in Fig. 7.

These results emphasize only the improvements brought to already optimized structures, because compared to a 70 turns Slinky-4 coil, positioned on the configuration 25-10-10-25 (all turns in one level), the improvement is even more significant (energy dissipated in the circuit is 25% higher and coil heating per pulse is 35% higher for this coil).

IV. CONCLUSION

This paper analysis the energetic efficiency of Slinky-4 coils used in magnetic stimulation. From the point of view of energy transfer from the coil to the target tissue, the circular coil and even the figure of 8 coil, also called Slinky-2 coil, are much more efficient than the other Slinky coils [4]. But since focality is also an important criterion to be considered when choosing a magnetic coil for a specific application, this paper analyses the optimal inner structure of a Slinky-4 coil, previously proved to be the one that produces an optimal focality of the induced electric field inside the tissue.

We establish that the radius of the coil's leafs should be about 30 mm, and analyze the role played by the space distribution of the turns on improving the energy transfer from the coil to the tissue. The conclusion is that optimization gains a reduction of over 15% in power consumption and of 8% in coil heating per pulse, which can be an important step forward in designing coils for repetitive magnetic stimulation.

Therefore, one can conclude that the application is the one that sets the best design for the magnetic coil, and there is no universal solution, suitable for all cases.

REFERENCES

- [1] J. Ruohonen and J. Virtanen, "Coil optimisation for magnetic brain stimulation," *Annals Biomed. Eng.*, vol. 25, 1997.
- [2] B. J. Roth and P. J. Basser, "A model of the stimulation of a nerve fiber by electromagnetic induction," *IEEE Trans. Biomed. Eng.*, vol. 37, 1990.
- [3] L. Cret and R. Ciupa, "Remarks on the optimal design of coils for magnetic stimulation," in *Proc. ISEM*, Bad Gastein, Austria, 2003, pp. 352–354.
- [4] L. Cret and M. Plesa, "Magnetic coils for localized stimulation of the central nervous system," *Acta Electrotehnica*. Cluj Napoca, Romania, 2006, pp. 114–117.
- [5] I. Trestian, O. Creț, L. Creț, and R. Tudoran, FPGA-based computation of the inductance of coils used for the magnetic stimulation of the nervous system biodevices. Funchal, Madeira, Portugal, Jan. 28–31, 2008, pp. 151–154.
- [6] P. L. Kalantarov and L. A. Teitlin, "Calculul Inductivităților". Editura Tehnica, Bucuresti, 1958.